

ITEM NO. 22

NTSB Materials Laboratory Factual Report

NATIONAL TRANSPORTATION SAFETY BOARD

Office of Research and Engineering
Materials Laboratory Division
Washington, D.C. 20594



August 7, 2001

MATERIALS LABORATORY FACTUAL REPORT

Report No. 01-080

A. ACCIDENT

Place : Nodaway, Iowa
Date : March 17, 2001
Vehicle : National Railroad Passenger Corporation
Operating Over Burlington Northern Santa Fe Railway
NTSB No. : DCA01-M-R003
Investigator : Cyril E. Gura, RPH-10

B. COMPONENTS EXAMINED

Four pieces of rail and four splice bars.

C. DETAILS OF THE EXAMINATION

The rail and splice bars were received from the south rail at the point of derailment of a westbound train. Three of the rail pieces, labeled "A" to "C" from east to west in figure 1, comprised a plug rail¹ in continuous welded rail (CWR), and the splice bars were from each end of the plug rail. The approximate lengths of pieces "A" to "C" were 29 inches, 74 inches, and 80.25 inches, respectively. Two transverse fractures were observed at locations "a" and "b". The fourth rail piece was a cut piece of the adjacent rail to the east and was joined by two splice bars to the eastern end of fractured rail piece "A". According to track maintenance records, a plug rail was installed on February 13, 2001 at the location of the derailment.

According to markings embossed on the rail, the rail was 132 pounds-per-yard controlled-cooled rail manufactured by Bethlehem Steel in February 1988. Stamped numbers indicated that the rail was from heat number 208N220 and was cut number S12. According to Bethlehem Steel records for that heat, the ladle treatment (stir station) and continuous casting were normal. Also, after 10 hours of controlled cooling, the rail temperature was 415 degrees Fahrenheit, which is within the 1991 American Railway Engineering Association (AREA)² specifications for controlled cooling of rail.

¹ Plug rail is used to describe a replacement rail segment that had been installed to repair a rail defect in continuously welded rail (CWR).

² *Manual for Railway Engineering*, American Railway Engineering Association, (1991) 4-2-6.

The vertical head loss was 0.188 inches, measured on pieces "B" and "C". Measurements of the gage face showed no wear. A dip was observed on the running surface at the east joint (between piece "A" and the adjacent piece of CWR rail). Over a 4-foot span, the maximum depth of the dip was approximately 0.13 inches. Marks consistent with wheel flange contact were observed on the field side splice bar at this joint, indicating a previous use. An orange-colored metal was observed on the field side of the adjacent rail heads near the joint, consistent with bond wire anchor locations. A remnant of a bond wire was also observed on the field side of the rail head near the west end of piece "C".

On piece "B", deformation of the field side of the rail base was observed at an area 20 to 28 inches west of fracture "a". This deformation was consistent with contact with a tie support plate. On the gage side of rail piece "B", deformation was observed on the lower portion of the side of the head within 45 inches east of fracture location "b". The deformation was consistent with sliding contact with an object moving downward relative to the rail head.

On piece "C", the head was damaged and the base was fractured on the gage side near the west end.

The east end of the gage side splice bar from the west joint was damaged consistent with receiving end damage. Circumferential marks were observed around the bolt holes, consistent with sufficiently torqued bolts.

Fracture Surface Examination

A view of the east fracture surface at location "a" is shown in figure 2. A portion of the fracture surface within the dashed-line boundary appeared relatively smooth with curving crack arrest lines, features consistent with fatigue. The fatigue features covered approximately 90 percent of the head area and emanated from an origin located 0.65 inches below the running surface and 0.01 inches toward the gage side of the centerline. A center portion of the fatigue region was noticeably smoother than the rest, having a diameter of approximately 0.5 inches centered on the origin. The remaining fracture surface outside the fatigue boundary was relatively rough with chevron marks pointing back toward the fatigue boundary, features consistent with overstress fracture initiating from the fatigue boundary. The west fracture surface at location "a" had similar features.

Deformation consistent with receiving rail end damage³ was observed on both sides of the fracture surface. On the east side, the deformation was on the upper side of the head within 0.13 inches below the running surface and within 0.97 inches east of the fracture surface. On the west side, the deformation was on the upper side of the head within 0.16 inches below the running surface and within 0.41 inches west of the fracture surface. Based on markings on the rail base, fracture "a" was determined to be located at the edge of a tie support with the centerline of the support located west of the fracture.

³ Receiving rail end damage is an impact deformation on the vertical face of a receiving rail end. It can occur when a misalignment or gap between two rails allows the wheel to drop below the surface of the delivering rail, and hammer against the end of the receiving rail as it rolls over the end corner of the rail.

A view of the east fracture surface at location "b" is shown in figure 3. A portion of the fracture surface within the dashed-line boundary appeared relatively smooth with curving crack arrest lines, features consistent with fatigue. The fatigue features covered approximately 80 percent of the head area and emanated from an origin located 0.625 inches below the running surface approximately on the centerline. A portion of the fatigue region was noticeably smoother than the rest, having a diameter of approximately 0.563 inches centered on the origin. The remaining fracture surface outside the fatigue boundary was relatively rough with chevron marks pointing back toward the fatigue boundary, features consistent with overstress fracture initiating from the fatigue boundary. No rail end damage was observed on the east fracture surface.

The west fracture surface features for location "b" were generally obliterated by post-fracture damage consistent with receiving rail end damage. The field and gage sides of the head were missing. The field side of the base was damaged with downward deformation, and a small piece was missing. Some crack arrest lines were observed on the fracture surface that mated with the east side of the fracture.

The origin area for the east side of the fracture at location "a" is shown at higher magnification in figure 4, appearing dark in the view shown. Crack arrest lines for the relatively smooth fatigue area were observed encircling the origin. The origin as viewed by scanning electron microscopy (SEM) at higher magnification is shown in figure 5, and a dashed line indicates the origin area boundary. The origin had some areas that appeared somewhat granular and other areas that appeared relatively flat. Secondary cracks were also observed in the origin area. Similar features were observed for the origin area at location "b".

Cross-Sectional Examination

A longitudinal cut was made adjacent to the origin at location "a", and the section was ground to a plane intersecting the origin and polished. The cross-section near the edge of the origin is shown in figures 6 to 8. The microstructure consisted of fine pearlite, as shown in figures 6 and 7. Longitudinally-oriented stringers of manganese sulfide were observed, and no evidence of manganese oxide was observed. Cracks were observed in the microstructure as shown in figure 7. The cracks were primarily intergranular with some transgranular regions. Another view of the origin is shown in figure 8, tilted to show both the origin and the polished and etched cross-section. No large inclusions were observed near the origin.

Macroetching

A transverse and a horizontal section of the rail from piece "B" were macroetched, and the results are shown in figures 9 to 11.⁴ In the transverse section, central web

⁴ The macroetched surfaces in figures 10 and 11 are shown magnified using a stereo microscope. In the 1991 AREA specifications, no inspection method was suggested for the initial examination of the macroetched surface (visual examination is the standard practice). However, if there is a question of the seriousness of an indication,

streaking was observed, and a small amount of streaking extended into the head, as indicated by the arrow in figure 9. Cracks, consistent with cracking associated with internal hydrogen precipitation, were observed in the center of the head as shown in figure 10. Similar cracks were also observed in the center of the base. The average crack length intersecting the transverse plane was 0.0049 inch, and the maximum length observed was 0.012 inch. In the horizontal section, similar cracks were observed, as shown in figure 11. The cracks were observed primarily in the transverse plane and often appeared to be associated with longitudinal inclusions, a feature typical of cracking associated with internal hydrogen precipitation. The average crack length intersecting the horizontal plane was 0.0054 inch, and the maximum length observed was 0.014 inch.

Hardness and Chemical Composition

Hardness was measured on the longitudinal vertical plane approximately 0.25 inches from the field side of the head. Average hardness measured 30.4 HRC (289 BHN). According to 1991 AREA specifications, the hardness should be greater than 285 BHN.

The chemical composition for elements specified in the 1991 AREA specifications was determined by Artech Testing, Chantilly, VA. The results are shown in the table. The result for carbon was within testing allowance limits, and the remaining elements were all within the specified limits.

Table: Chemical Composition for 132 Pound-per-Yard Rail

Element	Measured from piece "B" (Weight Percent)	1991 AREA specification (Weight Percent)
Carbon	0.83	0.72-0.82*
Manganese	0.91	0.80-1.10
Phosphorus	0.01	<0.035
Sulfur	0.01	<0.037
Silicon	0.12	0.10-0.50

*For carbon, the product analysis weight percent allowance is 0.04 above or below the specified chemical analysis limits.

According to the Metals Handbook,⁵ the hydrogen that leads to hydrogen flakes⁶ in steels such as rail steel typically comes from water vapor from the scrap, slag, or refractory linings on container vessels. Inclusions such as sulfides act as traps for the hydrogen. Having fewer inclusions to trap the hydrogen, low-sulfur steels are more susceptible to hydrogen flaking. The rail steel from this accident had a sulfur content of 0.01 weight percent, and the maximum sulfur content specified by the 1991 AREA specifications was 0.037 weight percent.

the sample could be examined using a stereo microscope up to 5X magnification, or a polished sample could be inspected up to 100X magnification.

⁵ Metals Handbook Volume 1, Properties and Selection: Irons, Steels, and High-Performance Alloys, 10th Edition, ASM International (1990) 716-717.

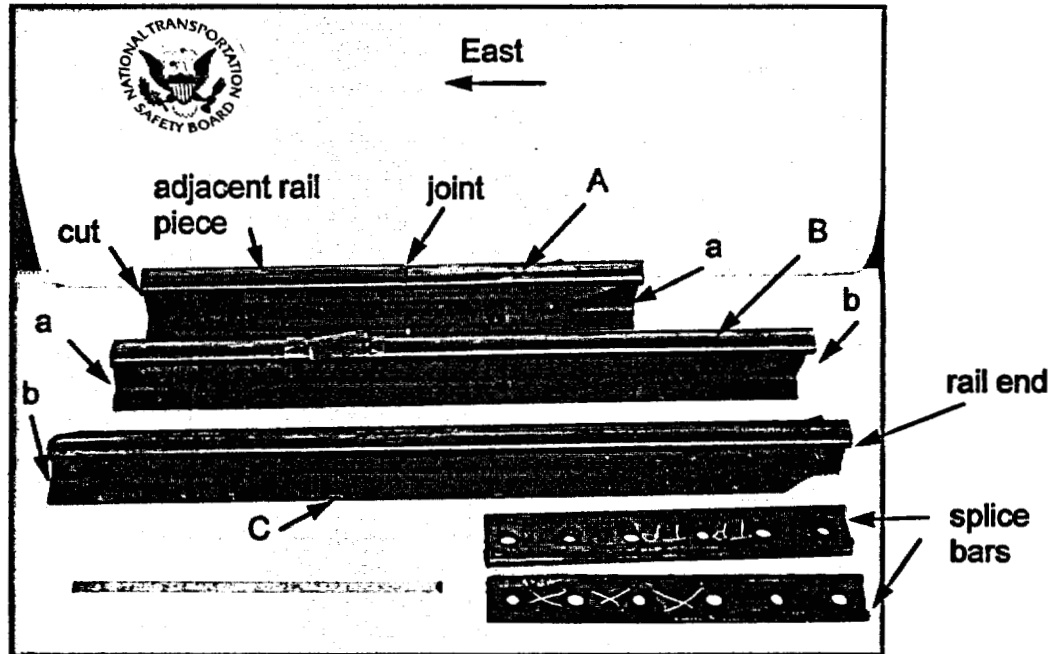
⁶ Flakes are cracks that typically form in heavy steel forgings and are caused by the precipitation of internal hydrogen. Typically, flakes appear as small bright elliptical areas on the fracture surface.

Ultrasonic Testing

The rail was tested using a 70-degree ultrasonic probe along the running surface. No crack indications were observed on rail pieces "A" or "C". However, in rail piece "B", three crack indications were detected near the east end. The ultrasonic testing indicated that two of the cracks were approximately 0.25 inches apart, with the smaller crack located 5.9 inches west of fracture "a" and the larger crack located 5.65 inches west of fracture "a". A transverse cut was made near the location of the smaller crack, leaving most of the head intact. The rail piece was then submerged in liquid nitrogen for a few minutes and then wedged open. The resulting fracture is shown in figure 12. A smooth region, consistent with fatigue, was observed on a portion of the fracture surface on a plane slightly offset from that of the rough overstress fracture. Based on the curvature of crack arrest lines in the fatigue region, the overstress fracture region appeared to intersect the fatigue region at a location just above the origin as indicated by arrows in figure 12. Dashed lines indicate the upper boundary of the fatigue region.

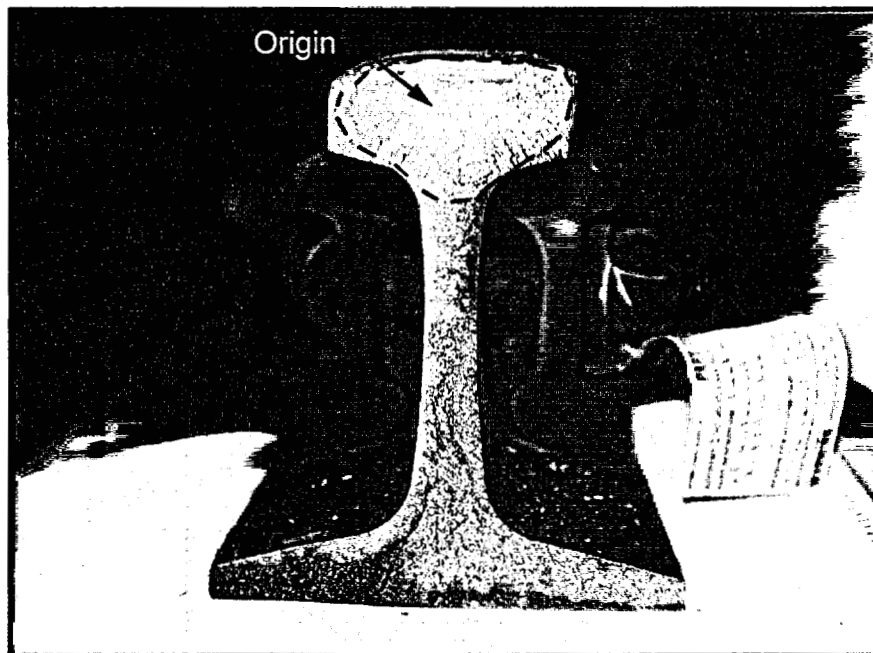
The ultrasonic testing indicated another crack located approximately 15.75 inches west of fracture "a". A 2.1-inch length of the rail was cut at that location, and the head was cut horizontally approximately 0.25 inches below the running surface. The lower piece was then fly cut with a milling machine at increments of 0.005 inches to 0.036 inches, and at each increment, the surface was ground to 600 grit, etched, examined visually, and tested with dye penetrant. No evidence of a crack was observed during the incremental examination.


Matthew R. Fox
Materials Engineer



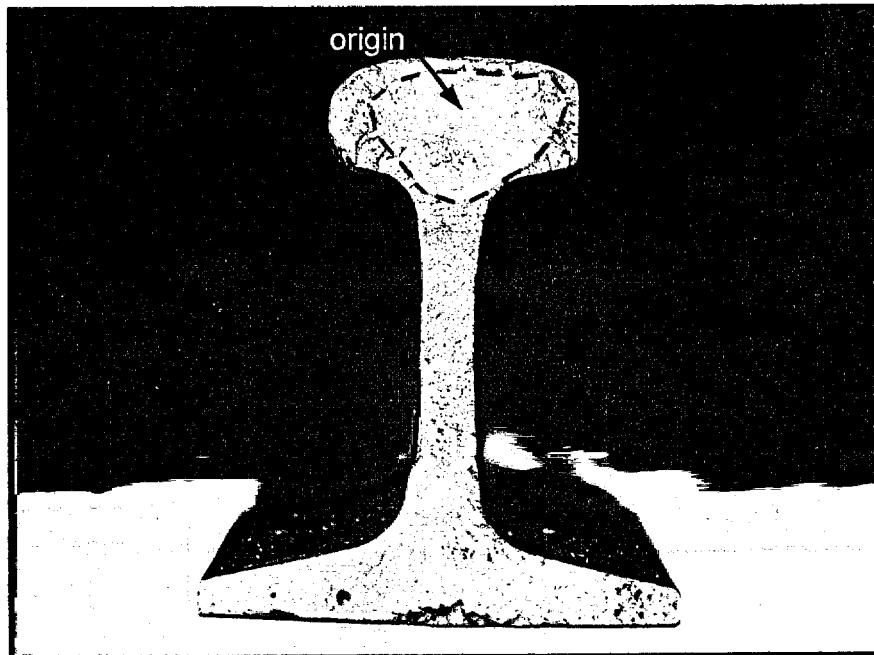
ImageNo:104A0195, Project No:A00182

Figure 1. Overall view of the submitted components, where three fractured pieces of rail are lettered "A" to "C" from east to west. Fracture locations are lettered "a" and "b" from east to west..



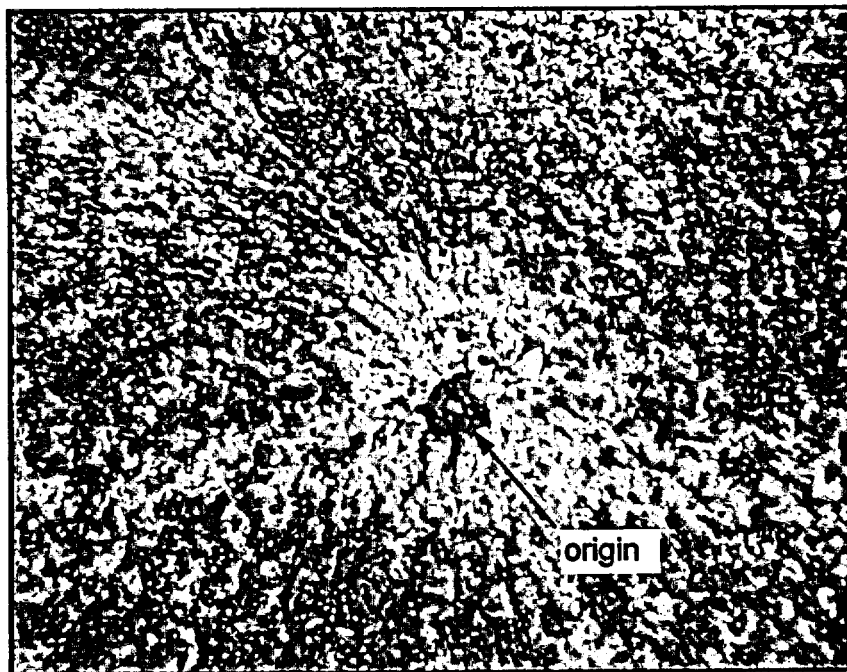
ImageNo: 104A0198, Project No:A00182

Figure 2. A view of the east fracture surface at location "a". An arrow and dashed line indicate the fatigue origin and boundary, respectively.



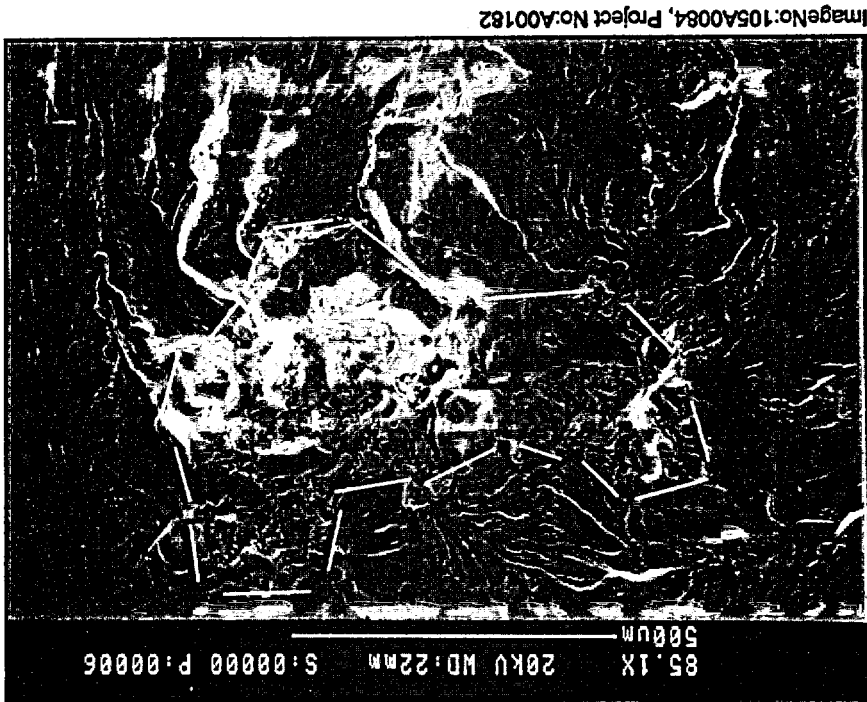
ImageNo:104A0200, Project No:A00182

Figure 3. A view of the east fracture surface at location "b". An arrow and dashed line indicate the fatigue origin and boundary, respectively.



ImageNo: 105A0034, Project No:A00182

Figure 4. A closer view of the origin area on the west fracture surface at location "a".



ImageNo:105A0084, Project No:A00182

Figure 5. The origin area on the west fracture surface at location "a" as viewed using SEM. A dashed line indicates the approximate boundary of the origin area.

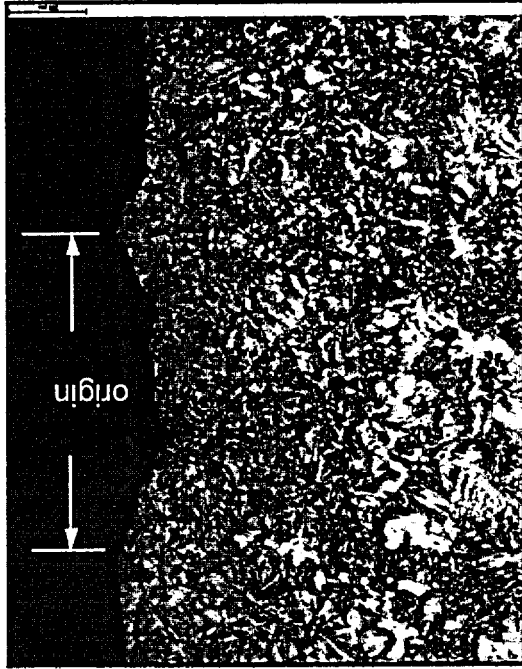


Figure 6. Cross-sectional view at the edge of the origin area on the west side of fracture location "a".

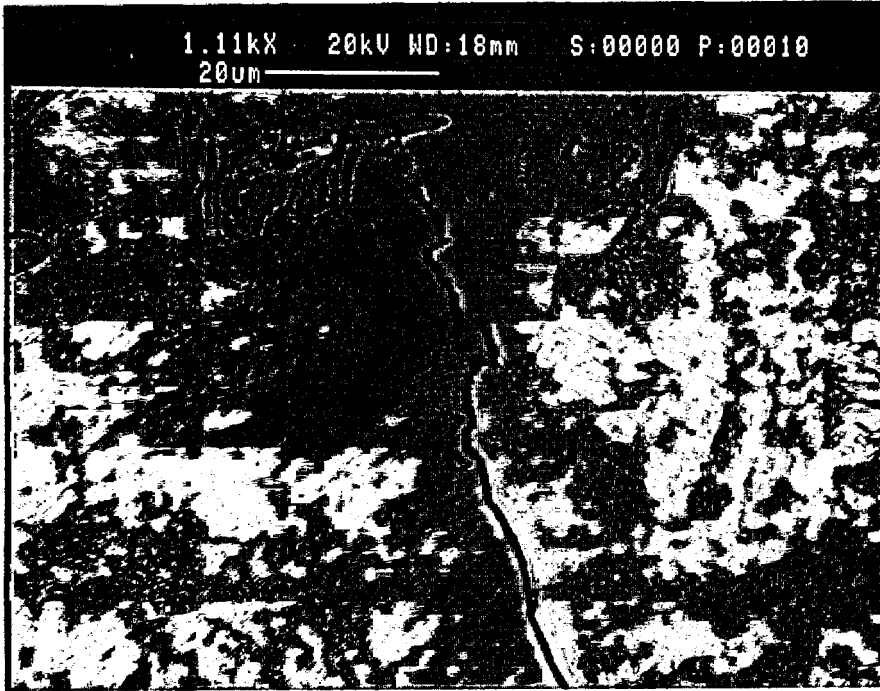


Figure 7. Cracks in the microstructure near the origin area on the west side of location "a".

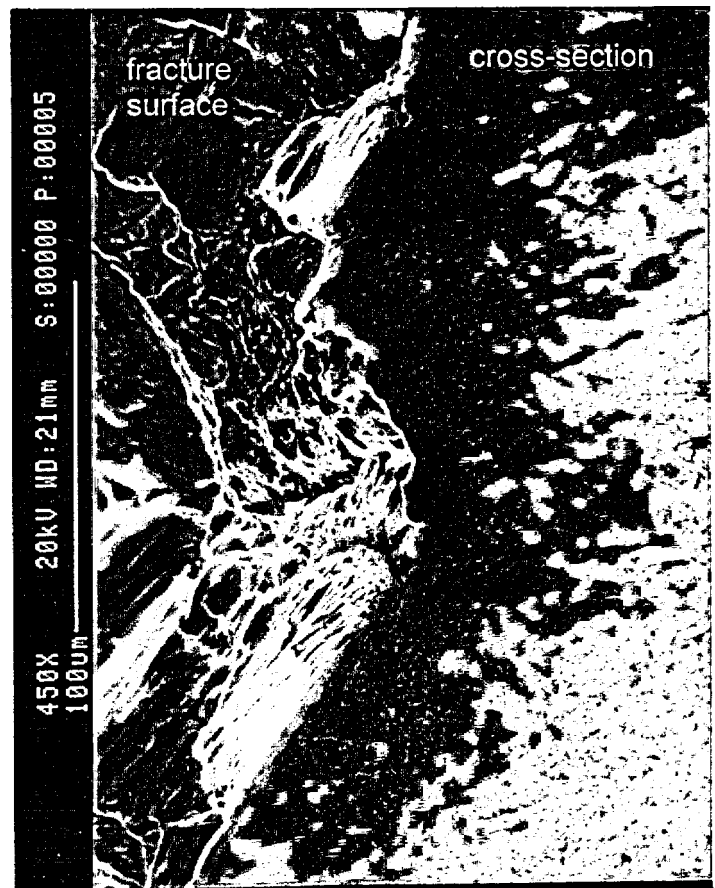
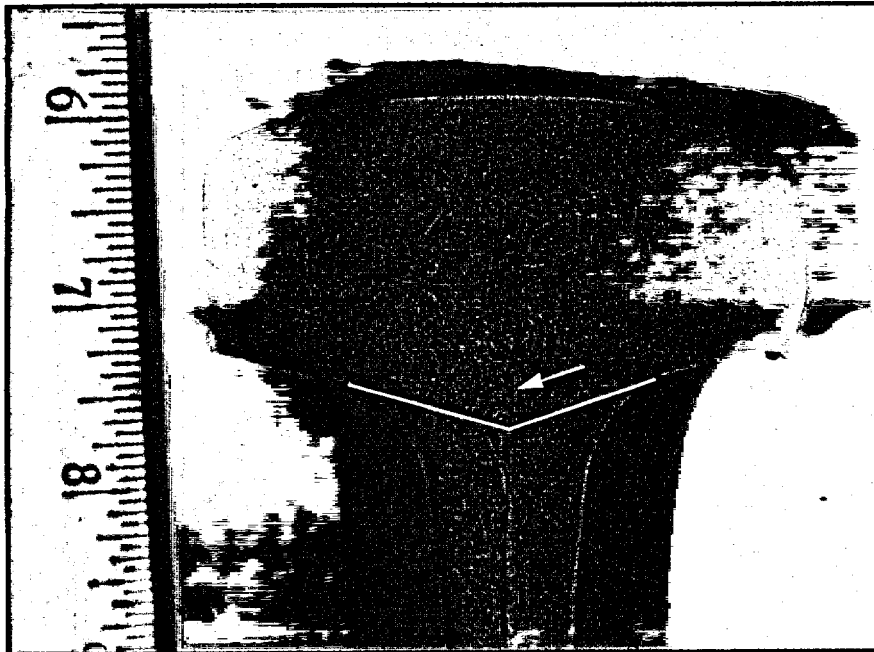
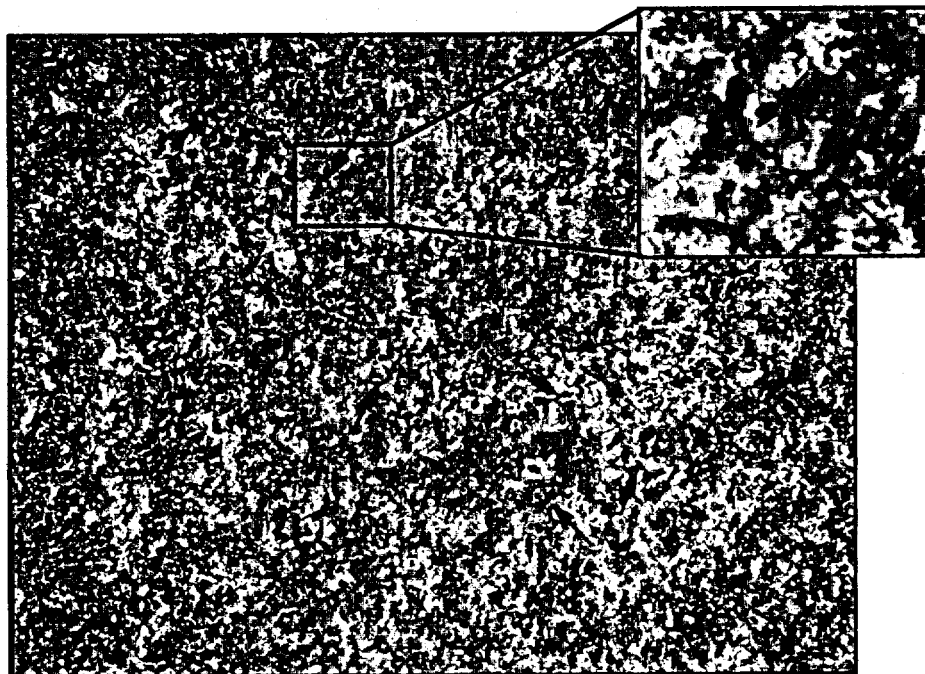


Figure 8. An view of the origin area using SEM at a tilted angle showing the origin area on the fracture surface and the adjacent microstructure in the cross-section.



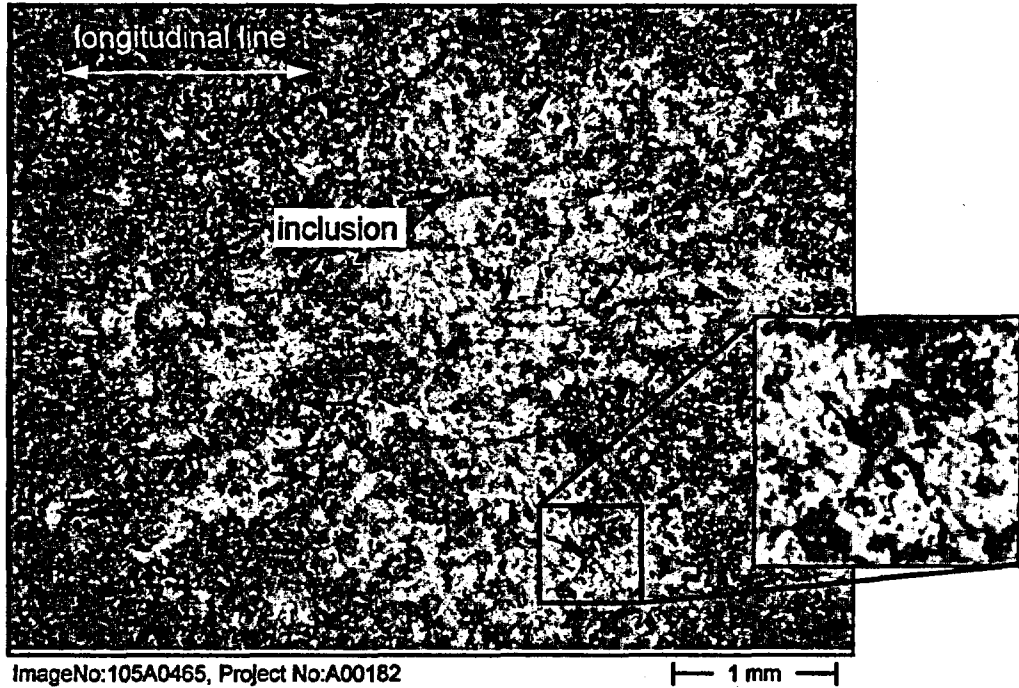
ImageNo:106A0266, Project No:A00182

Figure 9. A view of the macroetched rail head from piece "B". A solid line indicates the lower boundary of the head, and an arrow indicates some streaking observed in the head.



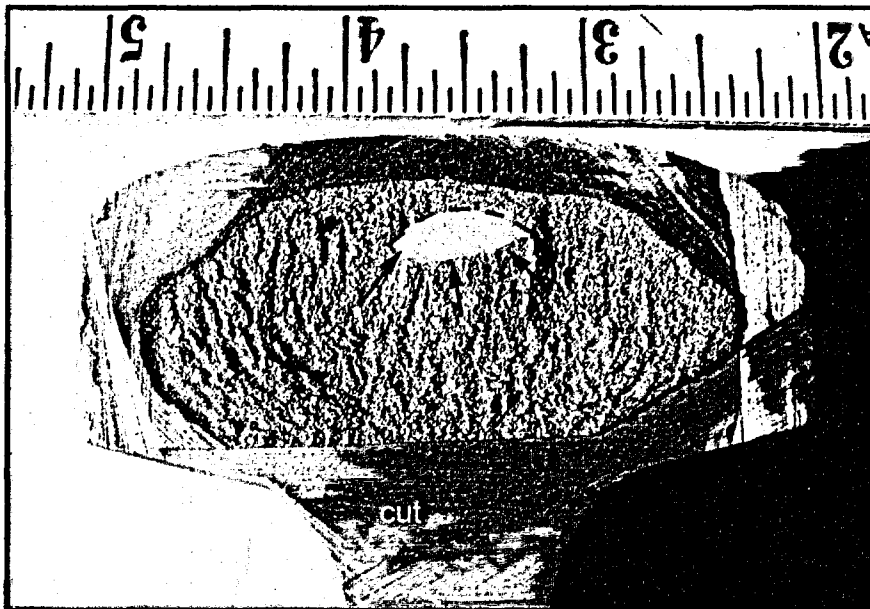
ImageNo: 105A0470, Project No:A00182

Figure 10. A closer view of the macroetched surface on the head shown in figure 9. Arrows indicate some of the observed cracks.



ImageNo:105A0465, Project No:A00182

Figure 11. A view of the macroetched horizontal section from piece "B". Unlabeled arrows indicate some of the observed cracks, and labeled arrows indicate inclusions.



ImageNo: 107A0151, Project No:A00182

Figure 12. The fracture surface of the rail piece fractured in the laboratory. Arrows indicate the intersection of the overstress fracture with the fatigue region, and a dashed line indicates the upper portion of the fatigue boundary.